


RESEARCH

Open Access



Transcriptional profiling of transport mechanisms and regulatory pathways in rat choroid plexus

Søren N. Andreassen¹, Trine L. Toft-Bertelsen¹, Jonathan H. Wardman¹, René Villadsen² and Nanna MacAulay^{1*} 

Abstract

Background: Dysregulation of brain fluid homeostasis associates with brain pathologies in which fluid accumulation leads to elevated intracranial pressure. Surgical intervention remains standard care, since specific and efficient pharmacological treatment options are limited for pathologies with disturbed brain fluid homeostasis. Such lack of therapeutic targets originates, in part, from the incomplete map of the molecular mechanisms underlying cerebrospinal fluid (CSF) secretion by the choroid plexus.

Methods: The transcriptomic profile of rat choroid plexus was generated by RNA Sequencing (RNAseq) of whole tissue and epithelial cells captured by fluorescence-activated cell sorting (FACS), and compared to proximal tubules. The bioinformatic analysis comprised mapping to reference genome followed by filtering for type, location, and association with alias and protein function. The transporters and associated regulatory modules were arranged in discovery tables according to their transcriptional abundance and tied together in association network analysis.

Results: The transcriptomic profile of choroid plexus displays high similarity between sex and species (human, rat, and mouse) and lesser similarity to another high-capacity fluid-transporting epithelium, the proximal tubules. The discovery tables provide lists of transport mechanisms that could participate in CSF secretion and suggest regulatory candidates.

Conclusions: With quantification of the transport protein transcript abundance in choroid plexus and their potentially linked regulatory modules, we envision a molecular tool to devise rational hypotheses regarding future delineation of choroidal transport proteins involved in CSF secretion and their regulation. Our vision is to obtain future pharmaceutical targets towards modulation of CSF production in pathologies involving disturbed brain water dynamics.

Keywords: Cerebrospinal fluid, Membrane transport, CSF secretion, RNA sequencing, RNAseq, Bioinformatics, Transcriptomics, Choroid plexus

Introduction

The brain is bathed in cerebrospinal fluid (CSF) that occupies the ventricular system, the subarachnoid space, and the interstitial space between structures and cells in the brain. The CSF serves to create buoyancy for the brain, to protect it from mechanical insult, and as a route by which metabolites, nutrients, and hormones can disperse within the brain [1]. The CSF is produced at a rate of 500 ml per day in adult humans [2], and the majority of the CSF secretion takes place across the choroid plexus

*Correspondence: macaulay@sund.ku.dk

¹ Department of Neuroscience, Faculty of Health and Medical Sciences, University of Copenhagen, Blegdamsvej 3, 2200 Copenhagen, Denmark
Full list of author information is available at the end of the article



© The Author(s) 2022. **Open Access** This article is licensed under a Creative Commons Attribution 4.0 International License, which permits use, sharing, adaptation, distribution and reproduction in any medium or format, as long as you give appropriate credit to the original author(s) and the source, provide a link to the Creative Commons licence, and indicate if changes were made. The images or other third party material in this article are included in the article's Creative Commons licence, unless indicated otherwise in a credit line to the material. If material is not included in the article's Creative Commons licence and your intended use is not permitted by statutory regulation or exceeds the permitted use, you will need to obtain permission directly from the copyright holder. To view a copy of this licence, visit <http://creativecommons.org/licenses/by/4.0/>. The Creative Commons Public Domain Dedication waiver (<http://creativecommons.org/publicdomain/zero/1.0/>) applies to the data made available in this article, unless otherwise stated in a credit line to the data.

[3], which is a specialized secretory tissue located in each of the ventricles. The choroid plexus consists of a monolayer of tight junction-connected epithelial cells, which rest on highly vascularized stroma with connective tissue [4].

A range of cerebral pathologies, i.e. hydrocephalus, stroke and subarachnoid hemorrhage, associate with elevated intracranial pressure (ICP). If left untreated, the brain tissue and the vasculature within compress, further reducing blood flow to the affected areas. Elevated ICP can occur following brain fluid accumulation arising either by reduced drainage of CSF following an obstruction in the brain fluid exit pathways or by hypersecretion of CSF, the latter of which has been observed in conditions such as choroid plexus hyperplasia, choroid plexus papilloma, and in a rodent model of posthemorrhagic hydrocephalus [5–7]. Elevated ICP is routinely treated by insertion of a ventriculo-peritoneal shunt or by a craniectomy [8, 9]. Although these are life-saving procedures, they are highly invasive and associated with severe side effects. Targeted and efficient pharmaceutical treatment aimed at reducing CSF secretion, and thus balancing the brain fluid content, is a desired addition to the clinical toolbox. However, such pharmaceutical approaches have, so far, generally failed due to intolerable side effects or lack of efficiency [10, 11].

Although the existence and production of CSF have been acknowledged for more than a century, the molecular mechanisms underlying this fluid secretion remain unresolved. Some choroidal transport mechanisms have been implicated in the CSF secretion, but their quantitative contribution and the molecular mechanisms by which the fluid is transported from the vascular compartment to the brain ventricles await determination [2, 3, 12]. Importantly, a complete map of the choroidal transport proteins may reveal other fluid-secreting transport mechanisms that could serve as future choroid plexus-specific pharmaceutical targets aimed at reducing CSF secretion in pathological conditions that would benefit from such treatments.

Here we performed transcriptomic analysis of rat choroid plexus from male and female rats and created a searchable database on the obtained transcriptomic profiles. To reveal putative future pharmacological targets, transport mechanisms and regulatory pathways were identified, ranked according to expression levels, and tied together in association networks.

Materials and methods

Experimental rats

This study conformed to the European guidelines and ethical regulations for use of experimental animals. The study utilizes 9-week-old Sprague Dawley rats (Janvier

Labs, France) of male and female sex. The rats were housed with 12:12 light cycle with access to water and food ad libitum in accordance with the guidelines of the Danish Veterinary and Food administration (Ministry of Environment and Food) and approved by the animal facility at the Faculty of Health and Medical Sciences, University of Copenhagen. The rats were anaesthetized with intraperitoneal injection of xylazine and ketamine (6 mg/ml and 60 mg/ml in sterile water, 0.17 ml per 100 g body weight (ScanVet, Fredensborg, Denmark)) prior to decapitation and tissue collection.

Isolation of choroid plexus and proximal tubules

Choroid plexus (from lateral and 4th ventricles) were isolated from five male and five female rats, pooled respectively and stored in RNAlater[®] (Sigma-Aldrich, St. Louis, Missouri, USA) at -80°C . Kidney tissue was collected from the male rats, minced, and subsequently digested for 25 min at 37°C in a table shaker at 850 rpm in collagenase solution containing 1 mg/ml collagenase (type II, Gibco[®], Grand Island, NY, USA) and 1 mg/ml pronase (Roche, Mannheim, Germany) in buffer solution containing (in mM): 140 NaCl, 0.4 KH_2PO_4 , 1.6 K_2HPO_4 , 1 MgSO_4 , 10 Na-acetate, 1 α -ketoglutarate, 1.3 Ca-glucuronate, 5 glycine, in addition to 48 mg/l aprotinin (trypsin inhibitor, Sigma-Aldrich, St. Louis, Missouri, USA) and 25 mg/l DNase I (grade II, Roche, Mannheim, Germany), pH 7.56. In five-minute intervals, 1 ml of the solution containing the kidney tissue was transferred to an eppendorf tube containing 1 ml cold buffer solution with 0.5 mg/ml bovine serum albumin (Sigma-Aldrich, St. Louis, Missouri, USA) and replaced by 1 ml collagenase solution. Proximal tubules were manually collected under a microscope, centrifuged at $600\times g$ for 5 min, and the pellet stored in RNAlater[®] at -80°C .

Fluorescence-activated cell sorting (FACS) of choroid plexus epithelial cells

Choroid plexus was isolated from 10 male rats, minced, and digested in collagenase (15 mg/ml collagenase (type II, Gibco[®], Grand Island, NY, USA) in artificial CSF (aCSF)-HEPES containing (in mM): 120 NaCl, 2.5 KCl, 3 CaCl_2 , 1.3 MgSO_4 , 1 NaH_2PO_4 , 10 glucose, 17 Na-HEPES, pH 7.56 for 30 min at 37°C in a table shaker at 800 rpm. The supernatant was removed after 5 min centrifugation ($600\times g$) and the pelleted cells were resuspended in aCSF-HEPES. The cells were triturated 20 times with a 1000 μl pipette and filtered through a 70 μm filter (pluriStrainer, Mini 70 μm , PluriSelect, Leipzig, Germany), prior to incubation with an anti-NKCC1 antibody with an extracellular epitope (1:200 in aCSF-HEPES, #ANT-071, Alomone Labs[™], Jerusalem, Israel) for 30 min at 4°C . The cells were pelleted ($600\times g$, 5 min)

and resuspended in secondary antibody (1:500 in aCSF-HEPES, Alexa Fluor[®] 647—A-21245, Invitrogen[™], Carlsbad, California, USA), in which it was kept for 20 min at 4 °C prior to centrifugation (600×g, 5 min) and resuspension in cold aCSF-HEPES. Cells were analyzed and sorted on a FACSAria Fusion flow cytometer (BD Biosciences, Lyngby, Denmark).

Immunohistochemistry

15 µl FACS suspension was placed on poly-D-lysine-coated coverslips for 30 min at room temperature, after which excessive liquid was removed and the attached cells covered with 4% paraformaldehyde in PBS for 15 min at room temperature. Coverslips were washed 3 times with 0.02% tween-20 in PBS (PBST) and permeabilized with PBST for 10 min at room temperature. Cells were treated with a blocking solution (4% normal goat serum (NGS) in PBST) for 1 h at 4 °C prior to exposure to primary antibody against AQP1 (1:400, #AQP-001, Alomone Labs[™], Jerusalem, Israel) at 4 °C O/N. Coverslips were washed with PBST and incubated with secondary antibody (1:700, A-11034, Alexa Fluor[®] 488, Invitrogen[™], Carlsbad, California, USA) and Phalloidin (1:400, A22287, Alexa Fluor[™] 647, Invitrogen[™], Carlsbad, California, USA) for 2 h at room temperature. Cells were washed and mounted onto microscope glass slides with ProLong[™] Gold Antifade Mountant with DAPI (P36935, Invitrogen[™], Carlsbad, California, USA).

RNA extraction and sequencing

The RNA extraction and library preparation were performed by Novogene Company Limited, UK with NEB Next[®] Ultra[™] RNA Library Prep Kit (NEB, USA) prior to their RNA sequencing (paired-end 150 bp, with 12 Gb output) on an Illumina NovaSeq 6000 (Illumina, USA).

Bioinformatics and computational analyses:

All program parameter settings for library building and mapping, together with all scripts for the gene annotation and analysis are available at <https://github.com/Sorennorger/MacAulayLab-RNAseq2>.

Although it remains unknown whether a certain transcript level cut-off represents physiological relevance, all analyses exclude genes transcribed at levels below a cut-off at 0.5 transcripts per million (TPM) [13]. Raw data are available at the National Center for Biotechnology Information (NCBI) Gene Expression Omnibus (GEO) database (accession number: GSE194236).

RNA sequencing analysis

The 150 base paired-end reads were mapped to reference genome (*Rattus norvegicus* Rnor_6.0 v.103) using Spliced Transcripts Alignment to a Reference (STAR) RNA-seq

aligner (v. 2.7.2a) [14]. The mapped alignment by STAR was normalized to TPM with RSEM (RNA-Seq by Expectation Maximization v. 1.3.3) [15]. Gene information was gathered with mygene (v3.1.0) python library [16–18], from which gene symbol, alias, and Gene Ontology (GO) terms [19–21] were extracted. Mitochondrial genes (seq-name: MT) were omitted from the reference genome prior to comparison of the kidney proximal tubule transcriptional profiles with that of the choroid plexus, since the greater abundance of these genes in the proximal tubule would skew the plasma membrane transporter expression comparison.

Cross-species comparison

The human choroid plexus transcriptome was obtained from GEO database (GSE137619, SRR10134643-SRR10134648) [22–24] and the mouse choroid plexus transcriptome was obtained from GEO (GSE66312, SRR1819706-SRR18197014) [25]. All samples were quality controlled with fastqc [26] and trimmed with Trimmomatic [27] (Slidingwindow 4:20, minimum length of 35 bp). The human and mouse samples, together with rat sample 3 (male), were mapped to the human reference genome (*Homo sapiens* GRCh38 v.104), the mouse reference genome (*Mus musculus* GRCm39 v.104), and rat reference genome (*Rattus norvegicus* Rnor_6.0 v.103) with STAR (v. 2.7.2a). The reference genome for rat, mouse, and human for the cross-species analysis only contained gene/transcripts of biotype ‘protein coding’. Mapped alignments were normalized to TPM with RSEM (v. 1.3.3) and the mean from the samples for human and mouse, respectively, were used for further analysis. Transcribed genes sharing gene name between the compared species (or their orthologue, collected from ensemble.org via biomart martview) were included in the cross-species comparison.

Category section

Gene lists of transporters, pumps, water and ion channels, and G protein-coupled receptors (GPCR) were collected from the ‘target and family list’ from Guide to Pharmacology [28–31]. Genes annotated as ‘transporters’ were employed to generate the list of membrane transporters and pumps whereas genes annotated as ‘voltage-gated ion channels’, ‘ligand-gated ion channels’, and ‘other ion channels’ were employed to generate the list of water and ion channels. To filter for plasma membrane proteins, the transporter and pump gene list was initially filtered to exclude the mitochondrial and vacuolar transport families SLC25, ATP5, and ATP6V, after which the transporter and channel lists were filtered based on associated GO terms; ‘integral component of plasma membrane’ or ‘plasma membrane’, but only included

genes annotated as ‘integral component of membrane’ or ‘transmembrane,’ but not annotated as ‘lysosome,’ ‘endosome membrane,’ ‘lysosomal,’ ‘mitochondrion,’ ‘mitochondrial,’ ‘golgi apparatus,’ ‘vacuolar,’ or ‘endoplasmic.’ Genes annotated as ‘GPCR’ were employed to generate the list containing GPCRs. Receptor tyrosine kinases (RTK) were gathered from Human Genome Organisation (HUGO) Gene Nomenclature Committee (HGNC) database [32], with the annotations ‘receptor tyrosine kinase’ including sub group ‘ephrin receptors’ and ‘ErbB family.’ The list of kinases was obtained from the Kyoto Encyclopedia of Genes and Genomes (KEGG) database [33–36] for entries of ‘EC 2.7.10.2’ (non-specific protein-tyrosine kinase), ‘EC 2.7.12’ (Dual-specificity kinases) with the two sub-categories, and ‘EC 2.7.11’ (Protein-serine/threonine kinases) with the 33 sub-categories. These three entries were collected with organism specific “rno” (*Rattus norvegicus*) filter. These kinases were filtered for protein kinases by GO terms: ‘protein kinase activity,’ ‘protein serine/threonine kinase activity,’ ‘protein serine kinase activity,’ ‘protein threonine kinase activity,’ ‘protein tyrosine kinase activity,’ ‘map kinase activity.’ Kinases involved solely with transcription or cell cycle modulation were subsequently excluded. Phosphatases were gathered from the KEGG database with entries EC 3.1.3 (Phosphoric Monoester Hydrolases) with 108 subcategories. The phosphatases were filtered for protein-interacting phosphatases by GO terms: ‘phosphoprotein phosphatase activity,’ ‘protein serine/threonine phosphatase activity,’ ‘protein serine phosphatase activity,’ ‘protein threonine phosphatase activity,’ and ‘protein tyrosine phosphatase activity.’ Phosphodiesterases (PDE) were collected based on gene name starting with ‘PDE.’ Cyclases were obtained from the KEGG database [33–36] entry numbers ‘EC 4.6.1.1’ (adenylate cyclase) and ‘EC 4.6.1.2’ (guanylate cyclase).

Network analysis

The network analysis was generated from protein–protein association tables from the String-database [37, 38] as a plugin for Cytoscape (v. 3.8.2) [39]. Firstly, full interaction tables were generated through a full protein query of every protein in the lists of transporters and pumps, water and ion channels, GPCRs, RTKs, kinases, phosphatases, PDEs and cyclases. Secondly, the tables were filtered for interaction between the ‘transporters and pumps’ and all the regulatory genes (lists of GPCRs, RTKs, kinases, phosphatases, PDEs, and cyclases). All interactions between regulatory proteins were discarded. The same was done for ‘water and ion channels.’ We only included protein–protein associations that were curated in a database or were demonstrated to interact experimentally. Thirdly, these interaction tables were loaded

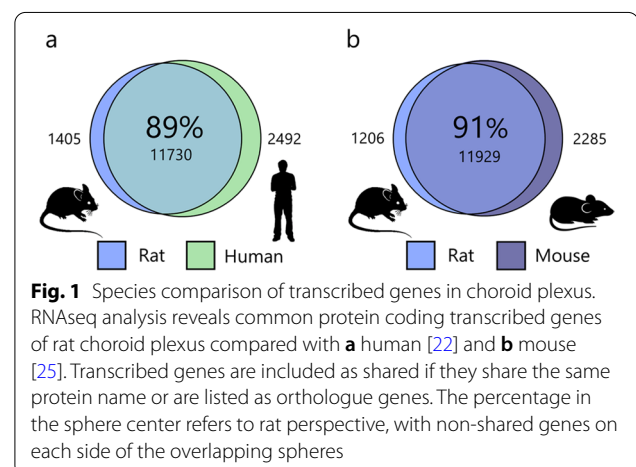
back into Cytoscape (v. 3.8.2) and modulated: Confidence score (from string-db) of 0.6–1 was used for genes from the list ‘transporter and pumps’ interactions and 0.7–1 was used for genes from the list ‘water and ion channels.’

Results

To characterize the choroid plexus ‘transportome,’ we obtained the transcriptomic profile of choroid plexus from adult male and female Sprague–Dawley rats by performing RNAseq of the tissue. The data are organized in a searchable webserver-based database (<https://cprnaseq.in.ku.dk/>) to allow search for genes of interest. The database encompasses the genes expressed in the choroid plexus, their expression level in TPM, and their alias (protein name, to the extent that this feature was available).

The transcriptomic profile of rat choroid plexus mimics those of mouse and human

To determine the species similarity of the choroid plexus transcriptomic profile, we compared that obtained from the rat (Additional file 1, sheet 1) to published versions of these obtained from human [22] and murine [25] choroid plexus. Notably, this species comparison illustrates whether or not the gene is present but does not confer quantitative comparison of the expression levels. The rat shares 89% of its choroidal protein-coding genes with that of the human choroid plexus, and 91% with that of mice (Fig. 1). These numbers may represent an underestimate, as some of the remaining genes might not be annotated with the shared name or as an orthologue, or may fall just above or below the cut-off level of 0.5 TPM. However, the 11% non-shared expressed genes in humans only account for 3.3% of the total transcripts and only 5.5% of these non-shared genes were annotated with ‘transport activity,’ meaning that only 0.1% are



transporters not shared with the rat. The 9% non-shared expressed genes for mouse account for 2.8% of the total transcripts, and only 0.1% was annotated as transporters. Such transcriptomic similarity suggests that the functional integrity is conserved among these organisms, and that the rat is an applicable animal model in which to determine physiological aspects, especially those that are membrane transport-related, of the choroid plexus.

Transport proteins highly expressed in choroid plexus may be involved in CSF secretion

To obtain a complete list of transport proteins expressed in the choroid plexus and their transcriptomic abundance, the RNAseq data were filtered for genes encoding transport proteins located in the plasma membrane (see Methods). Each gene was associated with its alias, and a description of the type of membrane transport protein. Some protein names and their function were well established, while other transport mechanisms expressed in choroid plexus appeared not fully characterized with no general agreement on a given alias or function. The lists were therefore manually curated according to the Universal Protein Resource (Uniprot) [40] and the Human Gene Database (Genecards) [41] to ensure that the widest accepted alias and function were associated with each gene name. The transport proteins are divided into

(i) coupled transporters and ATP-driven pumps and (ii) water and ion channels, and sorted according to their transcript abundance (Additional file 1, sheets 2 and 3). Tables 1 and 2 illustrate the 20 highest expressers in each category. Several of the transport proteins implicated in CSF secretion are found amongst these highly expressed transport proteins; different subunits of the Na⁺/K⁺-ATPase, the Na⁺,K⁺,2Cl⁻ cotransporter (NKCC1), aquaporin 1 (AQP1), and the HCO₃⁻ transporters NBCe2, NCBE, and AE2 [12, 42]. In addition, the lists present some additional transport proteins that could be envisaged to partake in CSF secretion, i.e. cation, anion and sulfate transporters (BOCT, BSAT1, SNAT1, SUT1, and MCT8, Table 1) in addition to various K⁺ and Cl⁻ ion channels (Table 2) with no prior association to CSF secretion. With such high relative expression in this tissue, these transport proteins are likely to serve a physiologically important function in choroid plexus, and could potentially be involved in CSF secretion.

The transcriptome of a pure fraction of choroid plexus epithelial cells is comparable to that of choroid plexus

The choroid plexus is a feather-like structure containing a monolayer of epithelial cells with centrally located vasculature, stroma, and immune cells. Most RNAseq studies of this tissue take advantage of the fact that the majority

Table 1 Highly transcribed transporters and pumps in choroid plexus

| Gene | Alias | TPM | Description | Rank | FACS rank | Female rank |
|----------|---------|------|--|------|-----------|-------------|
| SLC22A17 | BOCT | 2396 | Brain-specific organic cation transporter | 1 | 1 | 1 |
| ATP1B1 | NKAβ | 1553 | Na ⁺ /K ⁺ -ATPase β1 | 2 | 2 | 2 |
| FXYD1 | FXYD1 | 1076 | Na ⁺ /K ⁺ -ATPase γ1 | 3 | 3 | 3 |
| SLC4A5 | NBCE2 | 881 | Na ⁺ ,HCO ₃ ⁻ cotransporter | 4 | 7 | 4 |
| SLC4A2 | AE2 | 638 | Cl ⁻ /HCO ₃ ⁻ exchanger | 5 | 5 | 5 |
| SLC13A4 | SUT1 | 627 | Na ⁺ ,SO ₄ ²⁻ cotransporter | 6 | 6 | 7 |
| ATP1A1 | NKA.α1 | 623 | Na ⁺ /K ⁺ ATPase α1 | 7 | 4 | 6 |
| SLC31A1 | CTR1 | 469 | Cu ²⁺ transporter 1 | 8 | 9 | 8 |
| ATP2B3 | PMCA3 | 396 | Plasma membrane Ca ²⁺ ATPase | 9 | 15 | 11 |
| SLC16A2 | MCT8 | 380 | Monocarboxylate transporter 8 | 10 | 13 | 9 |
| SLC4A10 | NCBE | 325 | Na ⁺ , HCO ₃ ⁻ cotransporter | 11 | 26 | 12 |
| SLCO1C1 | BSAT1 | 301 | BBB-specific anion transporter 1 | 12 | 12 | 13 |
| SLC38A3 | SNAT3 | 298 | Na ⁺ -coupled neutral amino acid transporter 3 | 13 | 8 | 10 |
| SLC12A2 | NKCC1 | 268 | Na ⁺ , K ⁺ , 2Cl ⁻ cotransporter | 14 | 17 | 14 |
| ATP1B2 | NKA.β2 | 248 | Na ⁺ /K ⁺ ATPase β2 | 15 | 18 | 17 |
| ATP11A | ATP11A | 242 | Phospholipid-transporting ATPase | 16 | 23 | 19 |
| ATP1B3 | NKA.β3 | 236 | Na ⁺ /K ⁺ ATPase β3 | 17 | 10 | 15 |
| TMEM30A | TMEM30A | 229 | P4-ATPase flippase β subunit | 18 | 21 | 16 |
| SLC12A4 | KCC1 | 192 | K ⁺ , Cl ⁻ cotransporter | 19 | 11 | 18 |
| SLC20A2 | PIT2 | 182 | Na ⁺ -dependent PO ₄ ³⁻ transporter 2 | 20 | 16 | 21 |

RNAseq analysis revealing the 20 highest expressed genes encoding plasma membrane transporters and pumps in choroid plexus. TPM: transcripts per million; FACS rank: each gene's rank in the FACS sample; Female rank: rank in the choroid plexus from female rats

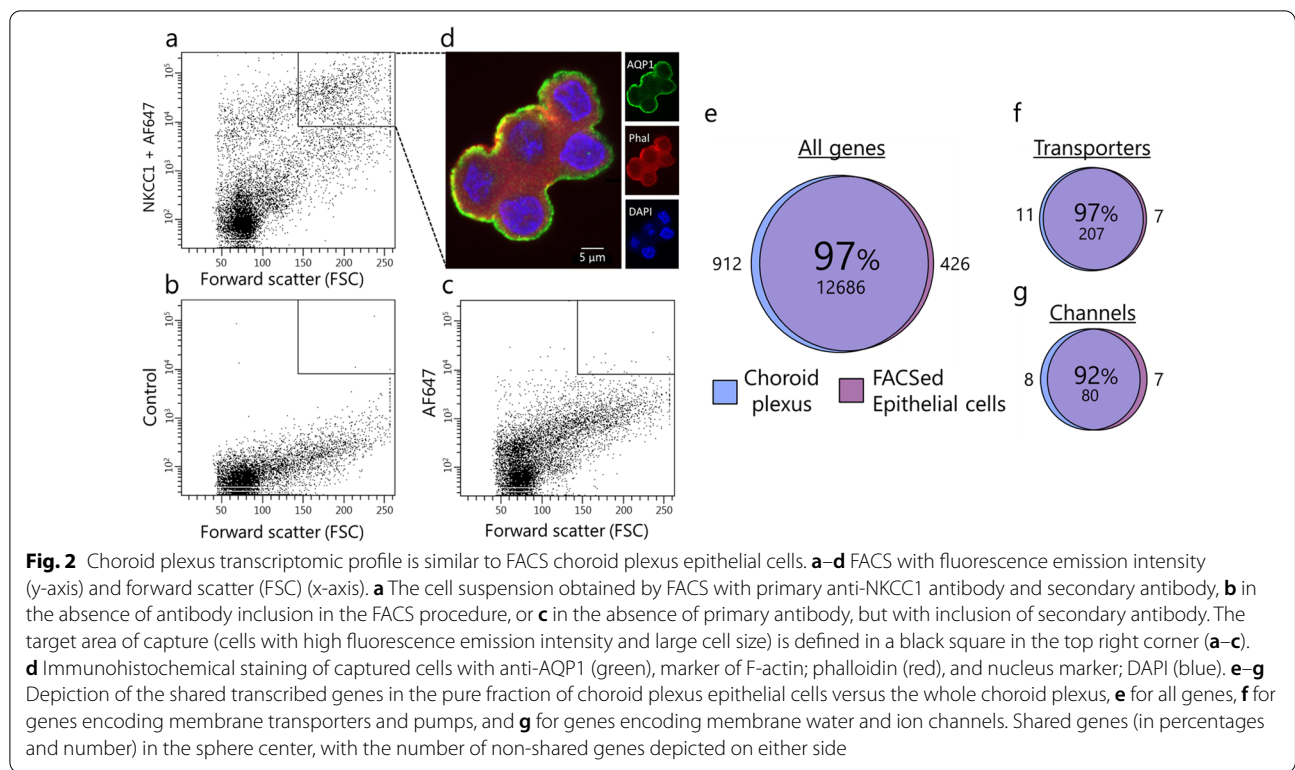
Table 2 Highly transcribed membrane channels in choroid plexus

| Gene | Alias | TPM | Description | Rank | FACS rank | Female rank |
|--------|--------|------|---|------|-----------|-------------|
| KCNJ13 | Kir7.1 | 1372 | Inwardly rectifying K ⁺ channel 7.1 | 1 | 2 | 1 |
| AQP1 | AQP1 | 721 | Aquaporin 1 | 2 | 1 | 2 |
| KCNK1 | TWIK-1 | 158 | Two pore domain K ⁺ channel | 3 | 3 | 3 |
| TRPM3 | TRPM3 | 137 | Transient receptor potential melastatin channel 3 | 4 | 7 | 4 |
| TRPV4 | TRPV4 | 92 | Transient receptor potential vanilloid channel 4 | 5 | 4 | 5 |
| ORAI1 | ORAI1 | 62 | Ca ²⁺ release-activated Ca ²⁺ modulator 1 | 6 | 5 | 6 |
| MCOLN1 | TRPML1 | 37 | Transient receptor potential mucolipin channel 1 | 7 | 6 | 7 |
| CLCN3 | CIC-3 | 34 | Voltage-gated Cl ⁻ channel 3 | 8 | 15 | 9 |
| KCNJ14 | Kir2.4 | 31 | Inwardly rectifying K ⁺ channel 2.4 | 9 | 55 | 8 |
| TRPM7 | TRPM7 | 30 | Transient receptor potential melastatin channel 7 | 10 | 18 | 12 |
| KCNQ1 | KV7.1 | 30 | Voltage-gated K ⁺ channel Kv7.1 | 11 | 9 | 10 |
| P2RX6 | P2X6 | 26 | Purinergic Receptor X6 | 12 | 8 | 11 |
| PKD2 | TRPP2 | 25 | Transient receptor potential polycystin channel 2 | 13 | 13 | 13 |
| KCNA1 | KV1.1 | 18 | Voltage-gated K ⁺ channel Kv1.1 | 14 | 43 | 20 |
| ORAI3 | ORAI3 | 17 | Ca ²⁺ release-activated Ca ²⁺ modulator 3 | 15 | 10 | 14 |
| KCNS1 | KV9.1 | 16 | Delayed rectifier voltage-gated K ⁺ channel Kv9.1 | 16 | 11 | 15 |
| KCNC3 | KV3.3 | 15 | Voltage-gated K ⁺ channel Kv3.3 | 17 | 21 | 18 |
| CLCN4 | CIC-4 | 14 | Voltage-gated Cl ⁻ channel 4 | 18 | 23 | 19 |
| GRIK5 | GluK5 | 13 | Kainate glutamate receptor 5 | 19 | 12 | 16 |
| GJB2 | Cx26 | 12 | Connexin26 | 20 | 14 | 22 |

RNAseq analysis revealing the 20 highest expressed genes encoding plasma membrane channels in choroid plexus. TPM; transcripts per million, FACS rank; each gene's rank in the FACS sample, Female rank; rank in the choroid plexus from female rats

of the cells in the tissue are choroid plexus epithelial cells [43, 44] and thus include the entire structure into the RNAseq procedure [45–49]. In this manner, some of the transcripts are anticipated to arise from other cell types than that of the choroid plexus epithelium. To resolve a putative discrepancy between a pure fraction of choroid plexus epithelial cells and that of the entire tissue, dissociated cells from acutely isolated choroid plexus were captured by FACS. In the choroid plexus, NKCC1 appears to be expressed exclusively on the luminal side of the epithelial cells [50–52] and FACS with the anti-NKCC1 antibody targeted to an extracellular epitope on this choroidal transport protein produced a fraction of highly fluorescent and large cells (Fig. 2A), which was absent in the FACS conducted in the absence of antibody (Fig. 2B) or with only the secondary antibody (Fig. 2C). Intact choroid plexus epithelial cells captured by FACS expressed AQP1 (Fig. 2D), which in the choroid plexus is expressed solely in the epithelial cells [53], demonstrating the epithelial origin of the captured cells. RNAseq analysis of the epithelial cells captured by FACS retrieved 97% of the genes detected in the entire choroid plexus structure (Fig. 2E). The 3% of the genes that were absent from the choroid plexus epithelial cells captured by FACS, were largely (>95% of the genes with cell type annotation) annotated primarily to cell types other than

epithelial cells [54, 55], such as cells of mesenchymal, endothelial, neuronal, immune, or glial origin, which reside in the choroid plexus structure [43]. The cell population obtained from the FACS procedure thus essentially represents choroid plexus epithelial cells. Choroid plexus epithelial cells captured by FACS displayed nearly identical transcriptomic profiles to that of the entire choroid plexus of choroidal transport proteins (97%, Fig. 2F) and channels (92%, Fig. 2G). The non-shared genes place around the cut-off TPM of 0.5 for both transporters and channels. More specifically, the transporters/pumps found amongst the top 20 highest expressers in the choroid plexus were all detected within the top 26 highest expressed transport proteins in the pure fraction of choroid plexus epithelial cells (Table 1). Such similarity was reproduced for choroid plexus membrane channels (except for the two ion channels K_{ir}2.4 and K_v1.1 that placed further down the list), Table 2. Complete lists of transporters and membrane channels detected in the purified choroid plexus epithelial cells are included as Additional file 1, sheets 4 and 5. We conclude that RNAseq analysis of the complete choroid plexus structure provides a representative quantitative identification of the membrane transport proteins expressed in the choroid plexus epithelial cells.



The choroid plexus expresses a wide range of membrane transporters

The solute carriers (SLC) represent a large group of membrane transport proteins containing more than 400 members divided amongst 66 families [56]. The 66 family names and transport functions were collected from the Bioparadigms SLC database [57, 58]. Of the 66 existing SLC families, transcripts of 52 of these gene families were detected in choroid plexus, and 44 of these coding for SLC family members residing in the plasma membrane (representing 63% of all choroid plexus transporter and pump transcripts in the plasma membrane). To obtain an overview of choroidal plasma membrane transport functions, the 44 SLC families detected in the choroid plexus plasma membrane were grouped into 11 supercategories according to similarities in transported substrates (Fig. 3, Additional file 1, sheet 6). The most abundantly expressed supercategory consisted of 31 electrolyte and bicarbonate transporters (six families, 2602 TPM) followed by seven organic an/cationic transporters (one family, 2581 TPM) and 19 large anion transporters (five families, 1929 TPM). These are followed by amino acid and neurotransmitter transporters (36 genes), various sugar transporters (17 genes), and vitamin transporters (6 genes), (Fig. 3 and Additional file 1, sheet 6). Notably, the choroid plexus expresses a wealth of metal transporters (dispersed among 22 genes from five families, 928

TPM, with zinc transporters as the most prominent (15 genes)), (Fig. 3 and Additional file 1, sheet 6). With such abundance and variety in transporter types, the choroid plexus obviously serves important physiological roles in transporting solutes across this epithelial layer, besides that serving as the CSF secreting machinery.

Female and male rats share choroid plexus transcriptomic profile

To verify the sex-specific transcriptomic profile of female versus male rat choroid plexus, we compared the expression profiles for choroid plexus obtained from each age-matched sex. The female choroid plexus shared 98% of the overall expression profile with the male choroid plexus (Fig. 4A), suggesting high functional similarity of the choroid plexus in the two sexes. Notably, the non-shared genes account for less than 0.1% of the total transcripts. To reveal potential sex-specific differences within the CSF secreting machinery, we compared the expression profile for membrane transport mechanisms. Choroid plexus obtained from the female rats shared 98% of the transcripts encoding transporters (Fig. 4B) and 95% of those encoding channels (Fig. 4C) with the male rat. The male 20 highest expressed genes were included in the top 21 highest expressed transporter genes in the female transporter category (Table 1) and in the top 22 highest expressed channel genes in the female channel category

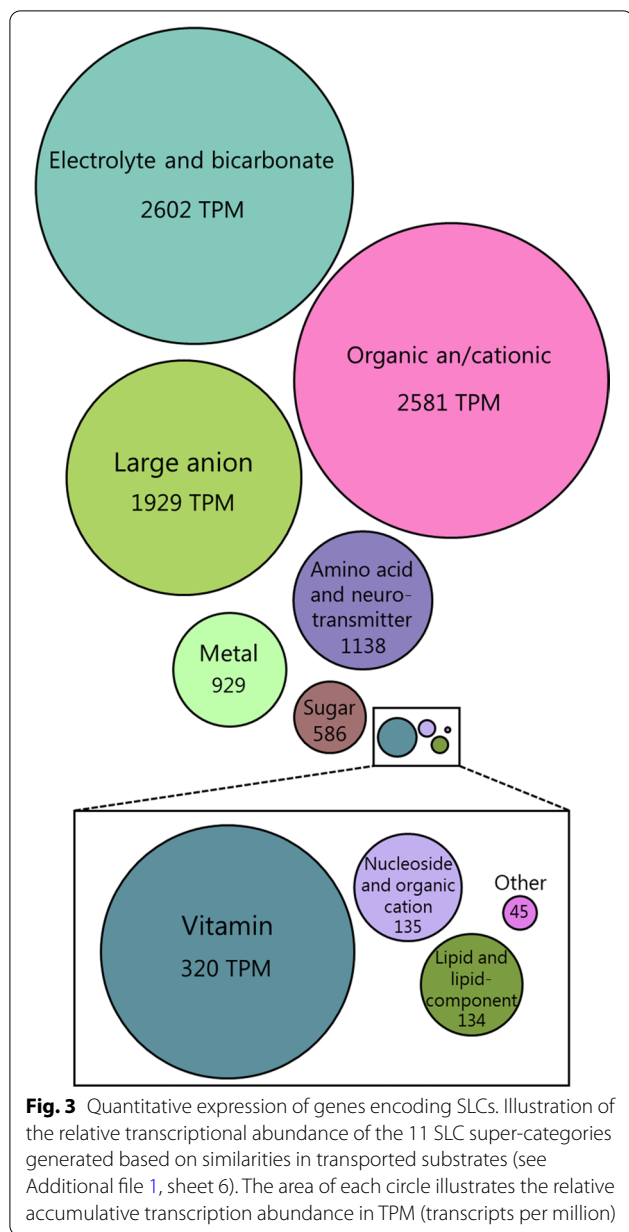


Fig. 3 Quantitative expression of genes encoding SLCs. Illustration of the relative transcriptional abundance of the 11 SLC super-categories generated based on similarities in transported substrates (see Additional file 1, sheet 6). The area of each circle illustrates the relative accumulative transcription abundance in TPM (transcripts per million)

(Table 2). Choroid plexus obtained from the two sexes thus shares high degree of expression profile similarity, with near-identical expression of abundant transport proteins. These data suggest a comparable choroid plexus CSF secreting machinery in female and male rats.

The choroid plexus transcriptome differs from that of another high-capacity isotonic fluid-transporting epithelium

To reveal possible transport protein candidates involved in fluid secretion across the choroid plexus, we obtained the transcriptomic profile of an epithelium of comparable

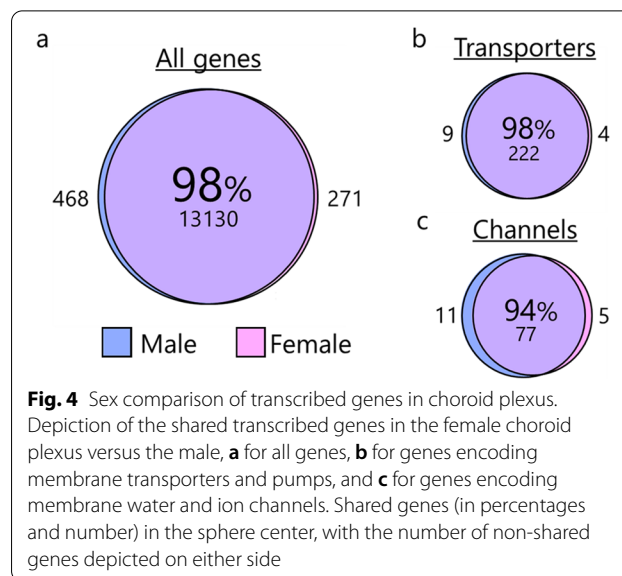
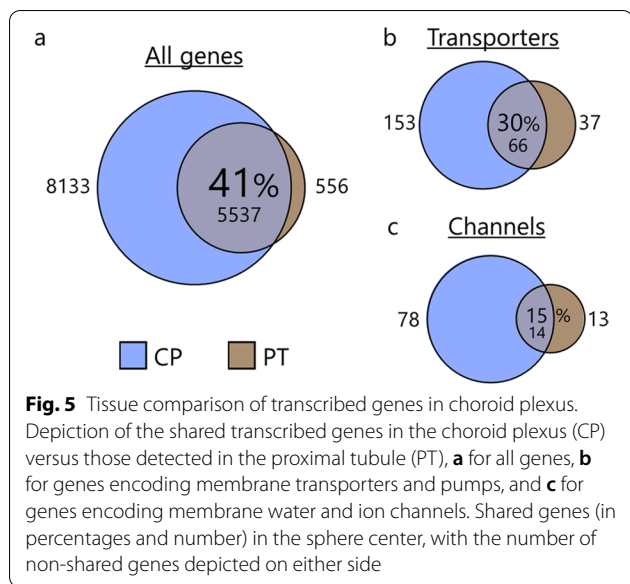


Fig. 4 Sex comparison of transcribed genes in choroid plexus. Depiction of the shared transcribed genes in the female choroid plexus versus the male, **a** for all genes, **b** for genes encoding membrane transporters and pumps, and **c** for genes encoding membrane water and ion channels. Shared genes (in percentages and number) in the sphere center, with the number of non-shared genes depicted on either side

isotonic fluid-transporting capacity to that of choroid plexus; the kidney proximal tubule [2]. The majority (91%) of the transcribed genes obtained in the proximal tubule were detected in the choroid plexus. However with the larger number of transcribed genes found in the choroid plexus, this common pool of transcribed genes amounted to only 41% of the choroidal expression profile (Fig. 5A). 64% of the transporter-encoding transcribed genes obtained from the proximal tubule were retrieved in the choroidal samples (in which proximal tubule transcribed genes represented 30%, Fig. 5B). In the channel category, the equivalent numbers were 52% of the proximal tubule transcribed genes being retrieved in the choroid plexus samples and 15% of the choroidal transcribed genes detected in the proximal tubule (Fig. 5C). Of the 20 highest expressed transporters/pumps (Table 3) and channels (Table 4) in the proximal tubule (see Additional file 1, sheets 7 and 8 for the complete lists), only 10 (transporters and pumps) and 10 (water and ion channels) genes were found in the choroid plexus (Tables 3 and 4). The Na⁺/K⁺-ATPase α1β1, AQP1, TRP channels, and some voltage-gated Cl⁻ channels present themselves as common transport mechanisms in the two tissues. Although the proximal tubule joins the choroid plexus in the ranks of high-capacity fluid-transporting epithelia, the molecular machinery driving the fluid secretion appears, at least in part, to rely on distinct transport mechanisms.

Receptors and intracellular modulators may be involved in regulation of CSF secretion

It is anticipated that CSF secretion is tightly regulated to ensure stable brain fluid dynamics and thus intracranial



pressure, although the regulatory control of CSF secretion is largely unresolved. To reveal which plasma membrane receptors are expressed in choroid plexus, all G protein-coupled receptors (GPCRs) and receptor tyrosine kinases (RTKs) expressed in choroid plexus were filtered from the RNAseq data set and listed according to

their expression levels (Additional file 1, sheets 9 and 10). Each gene was associated with its alias and a description of the type of receptor (if known). All receptors were manually curated [40, 41] to ensure that the widest accepted alias and function were associated with each gene name. Of the 20 highest expressed GPCRs (Table 5), the serotonin receptor 2C (HTR2C) figures at the top, and is accompanied by the endothelin receptor type B, the GABA_B receptor, corticotrophin releasing hormone receptor 2, several adhesion-associated receptors, and those belonging to the family of frizzled GPCRs. Notably, the list contains several orphan GPCRs (GPR146, GPR175, GPR107) without well-established ligands and functions, although GPR146 has been proposed as a receptor for insulin C-peptide [59], which in turn may regulate the Na⁺/K⁺ -ATPase [60]. Dominant amongst the receptor tyrosine kinase top expressers (Table 5) are receptors for growth factors (GF) of various kinds; fibroblast GF, platelet derived GF, vascular endothelial GF, and insulin/insulin-like receptors, in addition to various immune-related RTKs.

The receptors generally exert their function via intracellular signaling cascades promoting phosphorylation (kinases) or dephosphorylation (phosphatases) of target proteins such as transport proteins and transcriptional factors potentially promoting expression of select

Table 3 Highly transcribed transporters and pumps in proximal tubule

| Gene | Alias | TPM | Description | PT Rank | CP Rank |
|----------|---------|------|--|---------|---------|
| SLC7A13 | XAT2 | 7344 | Na ⁺ -independent aspartate/glutamate transporter | 1 | N/A |
| SLC3A1 | NBAT | 3113 | Neutral and basic amino acid transporter | 2 | 98 |
| SLC16A4 | MCT5 | 993 | Monocarboxylate transporter 5 | 3 | N/A |
| SLC13A1 | NAS1 | 384 | Na ⁺ , SO ₄ ²⁻ transporter 1 | 4 | N/A |
| FXSD2 | FXSD2 | 359 | Na ⁺ /K ⁺ ATPase γ2 | 5 | N/A |
| PDZD11 | PDZD11 | 279 | Plasma membrane Ca ²⁺ ATPase-interacting single-PDZ Protein | 6 | 30 |
| ABCG2 | BCRP | 164 | ATP binding cassette transporter G2 | 7 | 209 |
| SLC17A3 | NPT4 | 148 | Na ⁺ , PO ₄ ³⁻ transporter 4 | 8 | N/A |
| SLC5A12 | SMCT2 | 147 | Na ⁺ -coupled monocarboxylate transporter 2 | 9 | N/A |
| SLC31A1 | CTR1 | 136 | Cu ²⁺ transporter 1 | 10 | 8 |
| SLC51B | OSTB | 131 | Organic solute transporter β | 11 | N/A |
| ATP1B1 | NKA.β1 | 98 | Na ⁺ /K ⁺ -ATPase β1 | 12 | 2 |
| MAGT1 | MAGT1 | 72 | Mg ²⁺ transporter protein 1 | 13 | 58 |
| SLC34A1 | NPT2 | 67 | Na ⁺ , PO ₄ ³⁻ transporter 2 | 14 | N/A |
| SLC16A12 | MCT12 | 45 | Monocarboxylate transporter 12 | 15 | 42 |
| SLC22A6 | OAT1 | 29 | Organic anion transporter 1 | 16 | N/A |
| SLC22A2 | OCT2 | 25 | Organic cation transporter 2 | 17 | N/A |
| TMEM30A | TMEM30A | 24 | P4-ATPase flippase β subunit | 18 | 18 |
| SLC15A2 | PEPT2 | 22 | Peptide transporter 2 | 19 | 87 |
| SLC5A2 | SGLT2 | 22 | Na ⁺ , glucose cotransporter 2 | 20 | 137 |

RNAseq analysis revealing the 20 highest expressed genes encoding plasma membrane transporters and pumps in proximal tubule. TPM: transcripts per million; PT rank: each gene's rank in the proximal tubule sample; CP rank: each gene's rank in the choroid plexus sample; N/A: not applicable if the genes is transcribed below the applied cut-off of 0.5 TPM

Table 4 Highly transcribed membrane channels in proximal tubule

| Gene | Alias | TPM | Description | PT rank | CP rank |
|--------|-------------|-----|---|---------|---------|
| KCNJ16 | Kir5.1 | 235 | Inwardly rectifying K ⁺ channel 5.1 | 1 | N/A |
| KCNJ1 | Kir1.1 | 89 | Inwardly rectifying K ⁺ channel 1.1 | 2 | N/A |
| AQP1 | AQP1 | 48 | Aquaporin 1 | 3 | 2 |
| TRPV1 | TRPV1 | 15 | Transient receptor potential vanilloid channel 1 | 4 | N/A |
| GJB2 | Cx26 | 13 | Connexin 26 | 5 | 20 |
| AQP3 | AQP3 | 10 | Aquaporin 3 | 6 | N/A |
| AQP7 | AQP7 | 9 | Aquaporin 7 | 7 | N/A |
| TRPM7 | TRPM7 | 9 | Transient receptor potential melastatin channel 7 | 8 | 10 |
| GABRP | GABAR π | 9 | GABA(A) receptor π | 9 | N/A |
| MCOLN1 | TRPML1 | 8 | Transient receptor potential mucolipin channel 1 | 10 | 7 |
| MCOLN3 | TRPML3 | 7 | Transient receptor potential mucolipin channel 3 | 11 | N/A |
| CLCN4 | CIC-4 | 4 | Voltage-gated Cl ⁻ channel 4 | 12 | 18 |
| CFTR | CFTR | 4 | Cystic fibrosis transmembrane conductance regulator | 13 | N/A |
| CLCNKA | CICK1 | 3 | Voltage-gated Cl ⁻ channel | 14 | N/A |
| GJB1 | Cx32 | 3 | Connexin 32 | 15 | N/A |
| KCNJ15 | Kir4.2 | 2 | Inwardly rectifying K ⁺ channel 4.2 | 16 | 85 |
| CHRN1 | ACHB | 2 | Acetylcholine receptor β | 17 | 47 |
| PANX2 | Panx2 | 2 | Pannexin 2 | 18 | 40 |
| P2RX4 | P2X4 | 2 | Purinergic receptor X4 | 19 | 28 |
| GJA1 | Cx43 | 2 | Connexin 43 | 20 | 27 |

RNAseq analysis revealing the 20 highest expressed genes encoding plasma membrane channels in proximal tubule. TPM: transcripts per million; PT rank: each gene's rank in the proximal tubule sample; CP rank: each gene's rank in the choroid plexus sample, N/A: not applicable if the genes is transcribed below the applied cut-off of 0.5 TPM

transport proteins. To reveal such regulatory proteins expressed in choroid plexus, the RNAseq data were filtered for kinases and phosphatases, and the data manually curated to obtain alias and function (complete lists found as Additional file 1, sheets 11 and 12). The list of the 20 highest expressed kinases (Table 6) encompasses a large variety of kinases including MAP kinases, AKT kinases, and casein kinases. Interestingly, the Stk39 kinase (SPAK), which is the second highest expressed kinase in choroid plexus, is directly implicated in CSF secretion via its ability to activate NKCC1 [6]. The list of the 20 highly expressed phosphatases covers a variety of phosphatases encompassing both serine/threonine and tyrosine phosphatases (Table 6).

Some kinases are activated by cyclic nucleotides, such as cAMP required for PKA activation and cGMP required for PKG activation. The abundance of these cyclic nucleotides is regulated by cyclases and phosphodiesterases, the presence and activity of which could well modulate the CSF secretion in the choroid plexus [61–63]. The RNAseq data set was therefore filtered for the presence of these, and the 10 highest expressers amongst cyclases and phosphodiesterases are listed in Table 7, with the complete lists of manually

curated (for alias and function) genes included as Additional file 1, sheets 13 and 14.

Network analysis of choroid plexus

To obtain insight into potential physiologically relevant regulatory properties of the choroid plexus transport machinery, we built association networks of transporters/pumps (Fig. 6) and channels (Fig. 7) with the various choroidal receptors (GPCRs and RTKs) and intracellular messengers (kinases, phosphatases, PDEs, and cyclases). Such networks are obtained with a string database and provide links between the transport mechanisms and a regulatory factor, if such has been implied experimentally or in curated databases [64] in published work on any cell type or tissue. Most notably, various isoforms of protein kinase A (PKA) and MAP kinases (MAPK) associate with phosphorylation of different subunits of the Na⁺/K⁺-ATPase and the plasma membrane Ca²⁺-ATPase (PMCA), whereas the facilitative glucose transporter (GLUT4) and the Na⁺/H⁺ exchanger (NHE1) associate with a variety of different regulatory candidates (Fig. 6). The SPAK-mediated regulation of NKCC1 in choroid plexus [6, 65] is evidenced in the network association of these proteins along with the with-no-lysine kinases (WNK1-4), oxidative

Table 5 Highly transcribed plasma membrane receptors in choroid plexus

| Gene | Alias | TPM | Description |
|------------------------------------|---------|-----|---|
| G protein-coupled receptors | | | |
| HTR2C | 5-HT2C | 677 | Serotonin receptor 2C |
| EDNRB | ETB | 150 | Endothelin receptor type B |
| ACKR3 | ACKR3 | 78 | Atypical chemokine receptor 3 |
| FZD2 | FZ-2 | 76 | Frizzled-2 |
| SMO | FZ-11 | 62 | Frizzled-11 |
| GPR146 | GPR146 | 51 | G protein-coupled receptor 146 |
| ADGRG1 | GPR56 | 49 | Adhesion G protein-coupled receptor G1 |
| TPRA1 | GPR175 | 42 | G protein-coupled receptor 175 |
| FZD7 | FZ-7 | 36 | Frizzled-7 |
| GABBR1 | GABABR1 | 32 | GABA(B) receptor 1 |
| CRHR2 | CRHR2 | 28 | Corticotrophin releasing hormone receptor 2 |
| GPRC5C | GPRC5C | 27 | G protein-coupled receptor C5C |
| GPR107 | GPR107 | 23 | G Protein-Coupled Receptor 107 |
| ADGRA3 | ADGRA3 | 21 | Adhesion G protein-coupled receptor A3 |
| GPR137 | GPR137 | 20 | G protein-coupled receptor 137 |
| FZD6 | FZ-6 | 18 | Frizzled-6 |
| ADGRL1 | ADGRL1 | 16 | Adhesion G protein-coupled receptor L1 |
| LGR4 | GPR48 | 13 | G protein-coupled receptor 48 |
| ADGRF5 | ADGRF5 | 12 | Adhesion G protein-coupled receptor F5 |
| GPR162 | GPR162 | 12 | G protein-coupled receptor 162 |
| Receptor tyrosine kinases | | | |
| FGFR2 | FGFR-2 | 181 | Fibroblast growth factor receptor 2 |
| FGFR1 | FGFR-1 | 110 | Fibroblast growth factor receptor 1 |
| PDGFRA | PDGFRα | 83 | Platelet derived growth factor receptor α |
| NTRK2 | NTRK2 | 75 | Neurotrophic receptor tyrosine kinase 2 |
| DDR1 | DDR1 | 54 | Discoidin domain receptor tyrosine kinase 1 |
| TYRO3 | TYRO3 | 48 | TYRO3 protein tyrosine kinase |
| RYK | RYK | 38 | Receptor like tyrosine kinase |
| KDR | VEGFR2 | 25 | Vascular endothelial growth factor receptor 2 |
| INSR | INSR | 24 | Insulin receptor |
| PTK7 | PTK7 | 22 | Protein tyrosine kinase 7 |
| PDGFRB | PDGFRβ | 20 | Platelet derived growth factor receptor β |
| LMTK2 | LMTK2 | 17 | Lemur tyrosine kinase 2 |
| CSF1R | CSF1R | 17 | Colony-stimulating factor 1 receptor |
| TIE1 | TIE1 | 16 | Tyrosine kinase with immunoglobulin- and EGF like domains 1 |
| EPHB4 | EPHB4 | 16 | Ephrin receptor B4 |
| FLT1 | VEGFR1 | 15 | Vascular endothelial growth factor receptor 1 |
| AXL | AXL | 12 | AXL receptor tyrosine kinase |
| FGFR3 | FGFR-3 | 12 | Fibroblast growth factor receptor 3 |
| IGF1R | IGF1R | 10 | Insulin-like growth factor 1 receptor |
| TEK | TIE2 | 9 | Tyrosine kinase with immunoglobulin- and EGF like domains 2 |

RNAseq analysis revealing the 20 highest expressed genes encoding plasma membrane GPCRs (top) and receptor tyrosin kinases (bottom) in choroid plexus. TPM; transcripts per million

stress responsive kinase 1 (OSR1), and other cation-Cl⁻ cotransporters (Fig. 6). The different PKA isoforms associate with various ion channels as well, most prominently with voltage-gated K⁺ channels, while PKC

isoforms associate with the transient receptor potential vanilloid channel 4 (TRPV4) (Fig. 7), which modulates the rate of CSF secretion [66] and has been implicated in hydrocephalus development in a rat model of

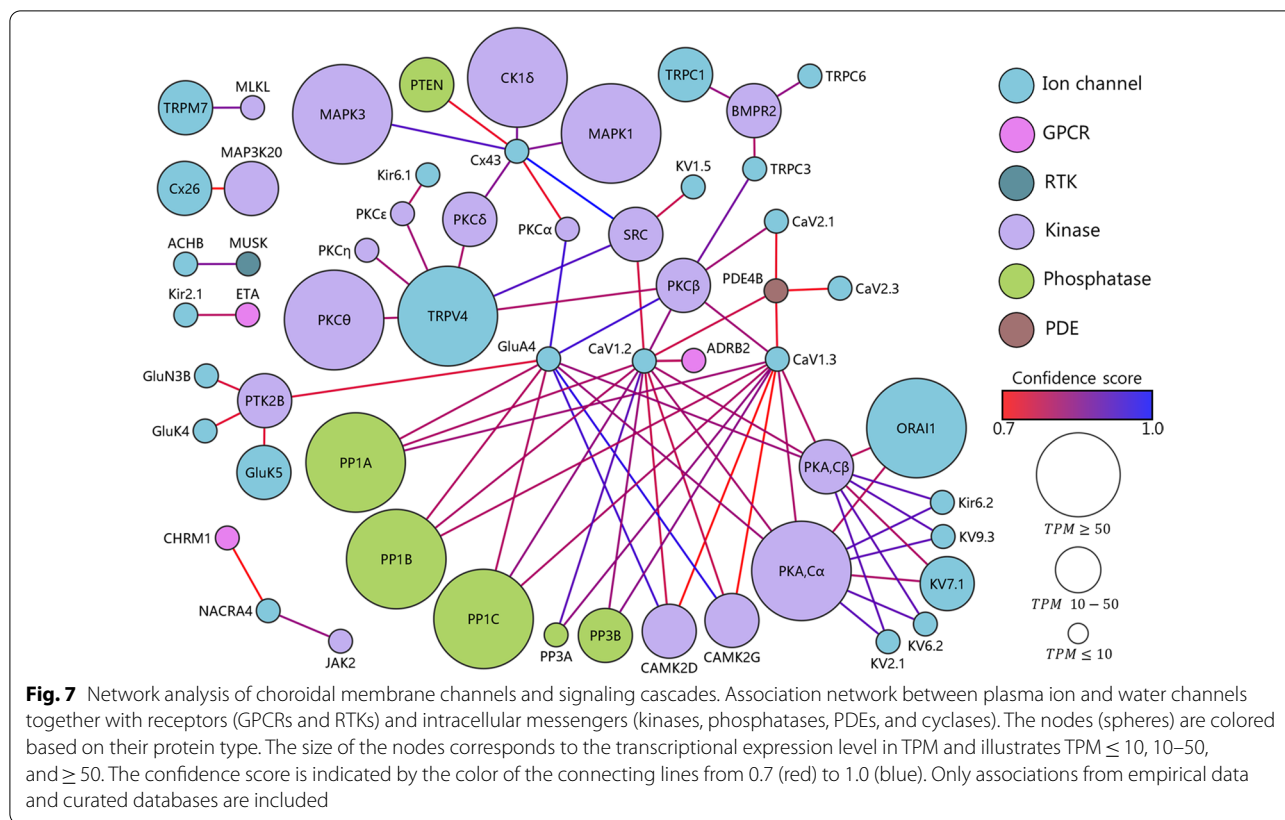
Table 6 Highly transcribed kinases and phosphatases in choroid plexus

| Gene | Alias | TPM | Description |
|---------------------|---------|-----|---|
| Kinases | | | |
| MAPK4 | MAPK4 | 324 | Mitogen-activated protein kinase 4 |
| STK39 | SPAK | 320 | STE20/SPS1-related proline-alanine-rich protein kinase |
| PINK1 | PINK1 | 196 | PTEN induced kinase 1 |
| SGK1 | SGK1 | 134 | Serum/glucocorticoid-regulated kinase 1 |
| CSNK1A1 | CK1α1 | 131 | Casein kinase 1, α1 |
| MAP2K2 | MAPKK2 | 123 | Mitogen-activated protein kinase kinase 2 |
| AKT1 | AKT1 | 121 | AKT serine/threonine kinase 1 |
| CSNK2A1 | CK2α1 | 121 | Casein kinase 2, α1 |
| CSNK1G2 | CK1 γ 2 | 109 | Casein kinase 1, γ2 |
| TGFBR2 | TGFBR2 | 102 | Transforming growth factor β receptor 2 |
| MAPK1 | MAPK1 | 92 | Mitogen-activated protein kinase 1 |
| DMPK | DM1PK | 90 | DM1 protein kinase |
| BCKDK | BCKDK | 87 | Branched chain ketoacid dehydrogenase kinase |
| MAPK3 | MAPK3 | 86 | Mitogen-activated protein kinase 3 |
| MAPKAP2 | MAPKAP2 | 75 | MAP kinase-activated protein kinase 2 |
| HIPK1 | HIPK1 | 75 | Homeodomain-interacting protein kinase 1 |
| PDK3 | PDK3 | 74 | Pyruvate dehydrogenase kinase 3 |
| GSK3A | GSK3A | 68 | Glycogen synthase kinase 3α |
| SGK3 | SGK3 | 66 | Serum/glucocorticoid-regulated kinase 3 |
| MAP2K1 | MAPKK1 | 65 | Mitogen-activated protein kinase kinase 1 |
| Phosphatases | | | |
| PPP2CB | PP2B | 268 | Protein phosphatase 2 Cβ |
| PTP4A2 | PTP4A2 | 179 | Protein tyrosine phosphatase 4A2 |
| PPP1CA | PP1A | 136 | Protein phosphatase 1 Ca |
| PPP5C | PP5 | 118 | Protein phosphatase 5 C |
| PPP1CC | PP1C | 105 | Protein phosphatase 1 Cγ |
| CTDSP1 | CTDSP1 | 102 | CTD small phosphatase 1 |
| PTPRA | PTPRA | 98 | Protein tyrosine phosphatase receptor α |
| PPP1CB | PP1B | 86 | Protein phosphatase 1 Cβ |
| PPP2CA | PP2A | 85 | protein phosphatase 2 Ca |
| CTDNEP1 | CTDNEP1 | 63 | CTD nuclear envelope phosphatase 1 |
| PTPN11 | PTPN11 | 57 | Protein tyrosine phosphatase non-receptor 11 |
| MTMR2 | MTMR2 | 55 | Myotubularin related protein 2 |
| PPM1F | PPM1F | 54 | Protein phosphatase, Mg ²⁺ /Mn ²⁺ dependent, 1F |
| DUSP14 | DUSP14 | 51 | Dual specificity protein phosphatase 14 |
| PPM1G | PPM1G | 48 | Protein phosphatase, Mg ²⁺ /Mn ²⁺ dependent, 1G |
| PGP | PGP | 47 | Phosphoglycolate phosphatase |
| MTMR6 | MTMR6 | 44 | Myotubularin related protein 6 |
| PTP4A1 | PTP4A1 | 43 | Protein tyrosine phosphatase 4A1 |
| PPP6C | PP6 | 41 | Protein phosphatase 6 C |
| PPP4C | PP4 | 40 | Protein phosphatase 4 C |

RNAseq analysis revealing the 20 highest expressed genes encoding protein kinases (top) and phosphatases (bottom) in choroid plexus. TPM: transcripts per million

genetically-induced hydrocephalus [67]. In addition, various highly expressed phosphatases associate with different ligand- and voltage-gated ion channels (Fig. 7). Altogether, such network analysis indicated a plethora

of potential regulatory pathways, some of which could be implicated in regulation of CSF secretion, or other physiological processes.



cells of epithelial origin [43]. These ranked lists of choroid plexus transport mechanisms, in addition, provided gene names of other highly expressed transport proteins, which could potentially contribute to CSF secretion, but may never have been investigated for such a function. Of interest could be the highly expressed cation and anion transporters (BOCT, BSAT1), both of which are detected in brain barrier tissues [69, 70]. BOCT is expressed widely across many brain cell types, whereas the BSAT1 is expressed predominantly in choroid plexus and other barrier cell types, i.e. endothelial cells and pericytes [71]. The transported substrate of the former remains elusive [69], whereas the latter is involved in the transport of thyroxine, for which the choroid plexus is renowned [70]. The Na⁺-coupled sulfate transporter (SUT-1), ranked as number 6 highest expressed amongst transporters and pumps, is virtually exclusively expressed in choroid plexus amongst brain cells [72] (with some expression in the vascular leptomeningeal cells [71]). MCT8 and SNAT3 are both highly expressed in choroid plexus epithelial cells, but also detected in other brain cell types, albeit the latter predominantly in barrier-related cells, such as vascular endothelial cells, pericytes and ependymal cells [71]. MCT8 is involved in thyroxine transport [73] while SNAT3 contributes to the high glutamine

content of the CSF [74]. None of these has, as of yet, been investigated for a potential implication in CSF secretion.

Comparison of the choroid plexus transcriptomic profile to that of another isotonic fluid-transporting epithelium of similar capacity, the kidney proximal tubules [2], revealed that choroid plexus expressed more than double the number of genes (~13,500 genes) compared to the proximal tubules (~6000 genes, [75, 76]). 64% of the transport protein transcripts detected in the proximal tubules were also expressed in the choroid plexus, but these only amounted to 30% of those detected within this transcript category in the choroid plexus, supporting the notion that the choroid plexus serves a variety of tasks other than CSF secretion, some of which include transepithelial solute transport. Amongst the genes encoding transport proteins transcribed in both fluid-transporting epithelia, surprisingly few placed among highly expressed genes in both tissues: the Na⁺/K⁺-ATPase $\alpha 1\beta 1$, AQP1, a voltage-gated Cl⁻ channel (ClC-4), in addition to two TRP channels (TRPML1 and TRPM7). Such similarity could suggest important roles of these particular transport proteins in the secretory processes (or regulation thereof) in these tissues [77–80], although, clearly, each epithelium appears to employ additional tissue-specific transport pathways to provide the transepithelial fluid

transport. Of interest, an isoform of the Na⁺-coupled glucose transporter (SGLT2; SLC5A2), which was previously annotated to sole expression in the proximal tubules [81], was here detected in the choroid plexus transcriptome, albeit at a lower relative expression level (6 TPM) than that observed in the proximal tubule sample (22 TPM). The choroidal transcript abundance of SGLT2 is confirmatory of its recently demonstrated protein expression in mouse and human choroid plexus [82, 83]. The proposed selective SGLT2 expression in the proximal tubules led to development of SGLT2 inhibitors as a selective treatment option for type 2 diabetes mellitus [84, 85]. Such approach may have to be reconsidered based on SGLT2 expression in choroid plexus (this study and [82, 83]), where the transport protein could potentially partake in CSF secretion, like its homologue, SGLT1, participates in fluid transport across the small intestine [86].

The families of solute carriers (the SLCs) were highly represented in the transportome of the choroid plexus (approximately 63% of all the plasma membrane transport and pump protein transcripts), with most of the existing families expressed in this tissue (52 out of 66). Choroid plexus SLC expression is developmentally regulated, with notable upregulation of amino acid transporter families during embryonic stages [45, 87]. Grouping these SLC families into super categories defined by their transported substrate, we demonstrate that the electrolyte/HCO₃⁻ and anion/cation transporters dominated at the transcript level. These were followed by amino acid, sugar, metal and vitamin transporters, in support of a role for choroid plexus in supplying the brain tissue with nutrients, micro-nutrients, and various co-factors [87, 88]. Notably, the choroid plexus is enriched in transcripts encoding metal transport proteins, with 22 genes dispersed among five different families of metal ion transporters. The choroidal expression of 15 different genes encoding various Zn²⁺ transporters of the efflux (SLC30; ZnT) and influx (SLC39, ZIP) types may serve to ensure transepithelial brain delivery of Zn²⁺ to various biochemical processes that are instrumental for proper brain development and function [87, 89, 90].

To reveal potential regulatory cascades involved in modulation of CSF secretion, we obtained lists of highly expressed plasma membrane receptors and signaling pathways expressed at the transcriptional level in choroid plexus. Amongst the GPCRs, the serotonin receptor of the 5-HT_{2C} type was expressed at fourfold higher abundance than the second-highest expressed receptor. The 5-HT_{2C} receptor is expressed on the luminal side of the choroid plexus epithelium [91] and its activation leads to G_q-dependent Ca²⁺ release from intracellular stores [92, 93], which subsequently promotes release of the insulin produced within the choroid plexus epithelium [93] and

may modulate choroidal ion channel activity [94] and the rate of CSF secretion [95, 96]. The endothelin receptor B appears as the second highest expressed GPCRs, with subtype A further down the list, in support of their protein expression in the choroid plexus [97]. Endothelin may reduce the rate of CSF secretion [98], possibly in part via its action on the choroidal blood flow [99]. Of the receptor tyrosine kinases, growth factor receptors dominate the list of highest expressers, with three members of the family of fibroblast growth factor (FGF) receptors on the top 20 list (and two of these at the top). FGF receptors are detected at the protein level in choroid plexus [100] and FGFs may be implicated in brain fluid homeostasis by their ability to modulate NKCC1 activity [101] and to induce ventriculomegaly in a rodent model upon prolonged intraventricular infusion, at least in part due to formation of fibrosis and collagen deposits in the CSF drainage paths [102]. The latter observation aligns with the diminished foramen magnum area observed in hydrocephalic children bearing mutations in the gene encoding FGFR2 [103].

Lists of highly expressed intracellular signaling molecules include various cyclases, phosphodiesterases, kinases and phosphates. The vast majority of these remains to be associated with CSF secretion or regulation thereof, but may provide valuable hints to pursue in future efforts to modulate CSF secretion pharmacologically without targeting the choroidal transporters, many of which are expressed in other cell types or epithelia in the body. The cyclase-coupled receptors for atrial natriuretic peptide (ANPR-A and ANPR-B) were both detected amongst the top 10 highest expressed cyclases in the choroid plexus, and previously demonstrated at the protein level in this tissue [104]. ANP, via its induction of cGMP formation, may [104] or may not [105] cause decreased CSF secretion, and altered choroid plexus ANP receptor abundance in various forms of experimental hydrocephalus could indicate involvement in brain fluid dynamics [106]. Also of interest is the placement of the Ste20-related proline/alanine-rich kinase, SPAK, as the second highest expressed kinase in choroid plexus. SPAK is implicated in regulation of the CSF-secreting NKCC1 [6, 65, 66] and figures prominently in our network analysis as associated with NKCC1 as well as other cation, Cl⁻ cotransporters (CCCs). Other choroidal kinases and phosphatases associate with different transport mechanisms, e.g. various isoforms of the Na⁺/K⁺-ATPase and the TRPV4 channel, and may provide novel paths to investigate in future determinations of choroid plexus transport and its regulation.

As potential limitations to our study, we acknowledge the possibility that the lists of transporters, receptors, and intracellular signaling molecules are not absolute,

as the information and annotation in the various databases, on which these are based, may be incomplete and with various levels of reliability. Accordingly, the volume activated anion channels of the LRRC8 family, which have been detected in rodent choroid plexus [107], were not included in the ion channel list from Gene Ontology in the first filtration step (see Methods), and are therefore not included in the list of choroidal ion channels. The filtration based on GO term annotation and manual curation was performed based on the available information and to the best of our knowledge. The network analysis is based on published work. Therefore, novel and unexplored connections between different transporters and their potential regulatory pathways are anticipated to be revealed by future research efforts. Lastly, transcript abundance may vary among the different choroid plexuses [25] and may not mirror the quantitative expression at the protein level, some of which have previously been reported [108]. In addition, it remains unresolved whether transport proteins with lesser mRNA abundance, at the protein level may remain functionally represented and physiologically relevant (e.g. $K_{v}1.3$ with low transcript abundance (this study and [25]), but detected at the functional level in isolated rodent choroid plexus [94]). Nevertheless, in the current study, we have created discovery tables of the transport mechanisms and regulatory pathways of the rat choroid plexus, and linked them via network analysis. We demonstrated high similarity between species (human and mouse) and sexes. The discovery tables provide semi-quantitative ranked lists of transport mechanisms that could participate in CSF secretion and suggest regulatory candidate genes that could be involved in their regulation. With these lists, we envision that researchers in the field may devise hypotheses regarding future quantification of transport mechanisms and their regulation, with the vision to obtain rational pharmaceutical targets for CSF production modulation in the pathologies involving disturbed brain water dynamics.

Abbreviations

aCSF: Artificial cerebrospinal fluid; ATP: Adenosine triphosphate; cAMP: Cyclic adenosine monophosphate; CCC: Cation Cl^{-} cotransporter; cGMP: Cyclic guanosine monophosphate; CSF: Cerebrospinal fluid; FACS: Fluorescence-activated cell sorting; FGF: Fibroblast growth factor; Genecards: Human gene database; GEO: Gene Expression Omnibus; GF: Growth factor; GO term: Gene Ontology term; GPCR: G protein-coupled receptor; HEPES: 4-(2-Hydroxyethyl)-1-piperazineethanesulfonic acid; HGNC: Gene Nomenclature Committee; HUGO: Human Genome Organisation; ICP: Intracranial pressure; KEGG: Kyoto Encyclopedia of Genes and Genomes; NCBI: National Center for Biotechnology Information; PBS: Phosphate-buffered saline; PDE: Phosphodiesterase; RNAseq: RNA sequencing; RSEM: RNA-Seq by Expectation Maximization; RTK: Receptor tyrosine kinase; SLC: Solute carrier; STAR: Spliced Transcripts Alignment to a Reference; TPM: Transcripts per million; Uniprot: Universal protein resource.

Supplementary Information

The online version contains supplementary material available at <https://doi.org/10.1186/s12987-022-00335-x>.

Additional file 1. Lists of RNAseq data.

Acknowledgements

We are grateful for the technical assistance from Trine Lind Devantier and Dagne Barbuskaite and for the valuable input on transcriptomics from Tune H Pers, Novo Nordic Center for Basic Metabolic Research, University of Copenhagen.

Author contributions

SNA and NM designed the research study, SNA, TLTB, RV, and JHW carried out the experiments, SNA, TLTB, RV, JHW, and NM analyzed the data, SNA and NM drafted the manuscript. All authors read and approved the final manuscript.

Funding

This project was funded by the Lundbeck Foundation (R276-2018-403 to NM and R303-2018-3005 to TLTB).

Availability of data and materials

The datasets used and/or analyzed during the current study are available from the corresponding author on reasonable request. Webserver database: <https://cprnaseq.in.ku.dk>. Scripts and data analysis: <https://github.com/Sorennorge/MacAulayLab-RNAseq2>. Raw data available at the NCBI GEO database with accession number: GSE194236 (<https://www.ncbi.nlm.nih.gov/geo/query/acc.cgi?acc=GSE194236>).

Declarations

Ethics approval and consent to participate

Animal experiments were in compliance with the European Community Council Directive 2010/63/EU on the Protection of Animals used for Scientific Purposes.

Consent for publication

Not applicable.

Competing interests

The authors declare that they have no competing interests.

Author details

¹Department of Neuroscience, Faculty of Health and Medical Sciences, University of Copenhagen, Blegdamsvej 3, 2200 Copenhagen, Denmark.

²Department of Cellular and Molecular Medicine, Faculty of Health and Medical Sciences, University of Copenhagen, Blegdamsvej 3, 2200 Copenhagen, Denmark.

Received: 21 February 2022 Accepted: 2 May 2022

Published online: 04 June 2022

References

- Redzic ZB, Preston JE, Duncan JA, Chodobski A, Szymdynger-Chodobska J. The choroid plexus-cerebrospinal fluid system: from development to aging. *Curr Top Dev Biol.* 2005;71:1–52.
- Damkier HH, Brown PD, Praetorius J. Cerebrospinal fluid secretion by the choroid plexus. *Physiol Rev.* 2013;93(4):1847–92.
- Hladky SB, Barrand MA. Fluid and ion transfer across the blood-brain and blood-cerebrospinal fluid barriers; a comparative account of mechanisms and roles. *Fluids Barriers CNS.* 2016;13(1):19.
- Solár P, Zamani A, Kubičková L, Dubový P, Joukal M. Choroid plexus and the blood-cerebrospinal fluid barrier in disease. *Fluids Barriers CNS.* 2020;17(1):35.

5. Hallaert GG, Vanhauwaert DJ, Loggh K, Van Broeck C, Den BE, Van Roost D, et al. Endoscopic coagulation of choroid plexus hyperplasia. *J Neurosurg Pediatr.* 2012;9(2):169–77.
6. Karimly JK, Zhang J, Kurland DB, Theriault BC, Duran D, Stokum JA, et al. Inflammation-dependent cerebrospinal fluid hypersecretion by the choroid plexus epithelium in posthemorrhagic hydrocephalus. *Nat Med.* 2017;23(8):997–1003.
7. Ducros A, Biousse V. Headache arising from idiopathic changes in CSF pressure. *Lancet Neurol.* 2015;14(6):655–68.
8. Ziebell M, Wetterslev J, Tisell M, Gluud C, Juhler M. Flow-regulated versus differential pressure-regulated shunt valves for adult patients with normal pressure hydrocephalus. *Cochrane Database Syst Rev.* 2013. <https://doi.org/10.1002/14651858.CD009706.pub2>.
9. Kofoed Månsson P, Johansson S, Ziebell M, Juhler M. Forty years of shunt surgery at Rigshospitalet, Denmark: a retrospective study comparing past and present rates and causes of revision and infection. *BMJ Open.* 2017;7(1): e013389.
10. Thurtell MJ, Wall M. Idiopathic intracranial hypertension (pseudotumor cerebri): recognition, treatment, and ongoing management. *Curr Treat Options Neurol.* 2013;15(1):1–12.
11. Piper RJ, Kalyvas AV, Young AM, Hughes MA, Jamjoom AA, Fouyas IP. Interventions for idiopathic intracranial hypertension. *Cochrane Database Syst Rev.* 2015. <https://doi.org/10.1002/14651858.CD003434.pub3>.
12. MacAulay N. Molecular mechanisms of brain water transport. *Nat Rev Neurosci.* 2021;22(6):326–44.
13. Abrams ZB, Johnson TS, Huang K, Payne PRO, Coombes K. A protocol to evaluate RNA sequencing normalization methods. *BMC Bioinform.* 2019;20(Suppl 24):679.
14. Dobin A, Davis CA, Schlesinger F, Drenkow J, Zaleski C, Jha S, et al. STAR: ultrafast universal RNA-seq aligner. *Bioinformatics.* 2013;29(1):15–21.
15. Li B, Dewey CN. RSEM: accurate transcript quantification from RNA-Seq data with or without a reference genome. *BMC Bioinformatics.* 2011;12:323.
16. MyGene.info. <https://mygene.info/>. Accessed 10 Sep 2021.
17. Xin J, Mark A, Afrasiabi C, Tsueng G, Juchler M, Gopal N, et al. High-performance web services for querying gene and variant annotation. *Genome Biol.* 2016;17(1):91.
18. Wu C, Macleod I, Su AI. BioGPS and MyGene.info: organizing online, gene-centric information. *Nucleic Acids Res.* 2013;41(Database issue):D561–5.
19. Mi H, Muruganujan A, Ebert D, Huang X, Thomas PD. PANTHER version 14: more genomes, a new PANTHER GO-slim and improvements in enrichment analysis tools. *Nucleic Acids Res.* 2019;47(D1):D419–26.
20. Carbon S, Ireland A, Mungall CJ, Shu S, Marshall B, Lewis S, et al. AmiGO: online access to ontology and annotation data. *Bioinformatics.* 2009;25(2):288–9.
21. Day-Richter J, Harris MA, Haendel M, Gene Ontology OBO-Edit Working Group, Lewis S. OBO-Edit—an ontology editor for biologists. *Bioinformatics.* 2007;23(16):2198–200.
22. Rodríguez-Lorenzo S, Ferreira Francisco DM, Vos R, van het Hof B, Rijnsburger M, Schrotten H, et al. Altered secretory and neuroprotective function of the choroid plexus in progressive multiple sclerosis. *Acta Neuropathol Commun.* 2020;8(1):35.
23. Edgar R, Domrachev M, Lash AE. Gene Expression Omnibus: NCBI gene expression and hybridization array data repository. *Nucleic Acids Res.* 2002;30(1):207–10.
24. Barrett T, Wilhite SE, Ledoux P, Evangelista C, Kim IF, Tomashevsky M, et al. NCBI GEO: archive for functional genomics data sets—update. *Nucleic Acids Res.* 2013;41(D1):D991–5.
25. Lun MP, Johnson MB, Broadbelt KG, Watanabe M, Kang Y, Chau KF, et al. Spatially heterogeneous choroid plexus transcriptomes encode positional identity and contribute to regional CSF production. *J Neurosci.* 2015;35(12):4903–16.
26. Andrews S. FastQC: A Quality Control Tool for High Throughput Sequence Data. 2010. Available from: <https://www.bioinformatics.babraham.ac.uk/projects/fastqc/>
27. Bolger AM, Lohse M, Usadel B. Trimmomatic: a flexible trimmer for Illumina sequence data. *Bioinformatics.* 2014;30(15):2114–20.
28. IUPHAR/BPS Guide to pharmacology. <https://www.guidetopharmacology.org/download.jsp>. Accessed 29 Oct 2021.
29. Alexander SP, Kelly E, Mathie A, Peters JA, Veale EL, Armstrong JF, et al. the concise guide to pharmacology 2019/20: transporters. *Br J Pharmacol.* 2019;176(Suppl 1):S397–493.
30. Alexander SP, Mathie A, Peters JA, Veale EL, Striessnig J, Kelly E, et al. The concise guide to pharmacology 2019/20: Ion channels. *Br J Pharmacol.* 2019;176(Suppl 1):S142–228.
31. Alexander SP, Christopoulos A, Davenport AP, Kelly E, Mathie A, Peters JA, et al. The concise guide to pharmacology 2019/20: G protein-coupled receptors. *Br J Pharmacol.* 2019;176(Suppl 1):S21–141.
32. HGNC Database, HUGO Gene Nomenclature Committee (HGNC), European Molecular Biology Laboratory, European Bioinformatics Institute (EMBL-EBI), Wellcome Genome Campus, Hinxton, Cambridge CB10 1SD UK. www.genenames.org. Accessed 15 Nov 2021.
33. KEGG; Kyoto Encyclopedia of Genes and Genomes. <https://www.kegg.jp/>. Accessed 1 Nov 2021.
34. Kanehisa M, Goto S. KEGG: kyoto encyclopedia of genes and genomes. *Nucleic Acids Res.* 2000;28(1):27–30.
35. Kanehisa M. Toward understanding the origin and evolution of cellular organisms. *Protein Sci.* 2019;28(11):1947–51.
36. Kanehisa M, Furumichi M, Sato Y, Ishiguro-Watanabe M, Tanabe M. KEGG: integrating viruses and cellular organisms. *Nucleic Acids Res.* 2021;49(D1):D545–51.
37. String database. <https://string-db.org/>. Accessed 2 Jan 2022.
38. Szklarczyk D, Gable AL, Lyon D, Junge A, Wyder S, Huerta-Cepas J, et al. STRING v11: protein-protein association networks with increased coverage, supporting functional discovery in genome-wide experimental datasets. *Nucleic Acids Res.* 2019;47(D1):D607–13.
39. Otasek D, Morris JH, Bouças J, Pico AR, Demchak B. Cytoscape automation: empowering workflow-based network analysis. *Genome Biol.* 2019;20(1):185.
40. The Universal Protein Resource. <https://www.uniprot.org>. Accessed 1 Nov 2021.
41. GeneCards: The Human Gene Database. <https://www.genecards.org>. Accessed 1 Nov 2021.
42. Oernbo EK, Steffensen AB, Khamesi PR, Toft-Bertelsen TL, Barbuskaite D, Vilhardt F, et al. Cerebrospinal fluid formation is controlled by membrane transporters to modulate intracranial pressure. *bioRxiv* 2021.12.10.472067.
43. Dani N, Herbst RH, McCabe C, Green GS, Kaiser K, Head JP, et al. A cellular and spatial map of the choroid plexus across brain ventricles and ages. *Cell.* 2021;184(11):3056–3074.e21.
44. Yang AC, Kern F, Losada PM, Agam MR, Maat CA, Schmartz GP, et al. Dysregulation of brain and choroid plexus cell types in severe COVID-19. *Nature.* 2021;595(7868):565–71.
45. Sathyanesan M, Girgenti MJ, Banasr M, Stone K, Bruce C, Guilchick E, et al. A molecular characterization of the choroid plexus and stress-induced gene regulation. *Transl Psychiatry.* 2012;2(7): e139.
46. Kant S, Stopa EG, Johanson CE, Baird A, Silverberg GD. Choroid plexus genes for CSF production and brain homeostasis are altered in Alzheimer's disease. *Fluids Barriers CNS.* 2018;15(1):34.
47. Stopa EG, Tanis KQ, Miller MC, Nikonova EV, Podtelezchnikov AA, Finney EM, et al. Comparative transcriptomics of choroid plexus in Alzheimer's disease, frontotemporal dementia and Huntington's disease: implications for CSF homeostasis. *Fluids Barriers CNS.* 2018;15(1):18.
48. Kratzer I, Liddelow SA, Saunders NR, Dziegielewska KM, Strazielle N, Ghersi-Egea JF. Developmental changes in the transcriptome of the rat choroid plexus in relation to neuroprotection. *Fluids Barriers CNS.* 2013;10(1):25.
49. Ek CJ, Nathanielsz P, Li C, Mallard C. Transcriptomal changes and functional annotation of the developing non-human primate choroid plexus. *Front Neurosci.* 2015;9:82.
50. Steffensen AB, Oernbo EK, Stoica A, Gerkau NJ, Barbuskaite D, Tritsaris K, et al. Cotransporter-mediated water transport underlying cerebrospinal fluid formation. *Nat Commun.* 2018;9(1):2167.
51. Plotkin MD, Kaplan MR, Peterson LN, Gullans SR, Hebert SC, Delpire E. Expression of the Na(+)-K(+)-2Cl- cotransporter BSC2 in the nervous system. *Am J Physiol.* 1997;272(1 Pt 1):C173–83.
52. Praetorius J, Nielsen S. Distribution of sodium transporters and aquaporin-1 in the human choroid plexus. *Am J Physiol Cell Physiol.* 2006;291(1):C59–67.

53. Speake T, Freeman LJ, Brown PD. Expression of aquaporin 1 and aquaporin 4 water channels in rat choroid plexus. *Biochim Biophys Acta*. 2003;1609(1):80–6.
54. PanglaoDB. <https://panglaoDB.se/>. Accessed 6 Jan 2022.
55. Franzén O, Gan LM, Björkegren JLM. PanglaoDB: a web server for exploration of mouse and human single-cell RNA sequencing data. Database. 2019. <https://doi.org/10.1093/database/baz046>.
56. Perland E, Fredriksson R. Classification systems of secondary active transporters. *Trends Pharmacol Sci*. 2017;38(3):305–15.
57. Bioparadigms: Advanced Biomedical Knowledge. <http://slc.bioparadigms.org/>. Accessed 12 Dec 2021.
58. Hediger MA, Cléménçon B, Burrier RE, Bruford EA. The ABCs of membrane transporters in health and disease (SLC series): introduction. *Mol Aspects Med*. 2013;34(2–3):95–107.
59. Yosten GL, Kolar GR, Redlinger LJ, Samson WK. Evidence for an interaction between proinsulin C-peptide and GPR146. *J Endocrinol*. 2013;218(2):B1–8.
60. Hills CE, Brunskill NJ. Intracellular signalling by C-peptide. *Exp Diabetes Res*. 2008;2018:635158.
61. Deng QS, Johanson CE. Cyclic AMP alteration of chloride transport into the choroid plexus-cerebrospinal fluid system. *Neurosci Lett*. 1992;143(1–2):146–50.
62. Nilsson C, Lindvall-Axelsson M, Owman C. Neuroendocrine regulatory mechanisms in the choroid plexus-cerebrospinal fluid system. *Brain Res Brain Res Rev*. 1992;17(2):109–38.
63. Rudman D, Hollins BM, Lewis NC, Scott JW. Effects of hormones on 3', 5'-cyclic adenosine monophosphate in choroid plexus. *Am J Physiol*. 1977;232(4):E353–7.
64. von Mering C, Jensen LJ, Snel B, Hooper SD, Krupp M, Foglierini M, et al. STRING: known and predicted protein-protein associations, integrated and transferred across organisms. *Nucleic Acids Res*. 2005;33(Database issue):D433–7.
65. Zhang J, Bhuiyan M, Zhang T, Karimiy J, Wu Z, Fiesler V, et al. Modulation of brain cation-Cl⁻ cotransport via the SPAK kinase inhibitor ZT-1a. *Nat Commun*. 2020;11(1):78.
66. Toft-Bertelsen TL, Barbuskaite D, Heerfordt EK, Lolansén SD, Andreasen SN, Rostgaard N, et al. Lysophosphatidic acid, a CSF marker in posthemorrhagic hydrocephalus that drives CSF accumulation via TRPV4-induced hyperactivation of NKCC1. *bioRxiv* 2022.01.24.477507.
67. Hochstetler AE, Smith HM, Preston DC, Reed MM, Territo PR, Shim JW, et al. TRPV4 antagonists ameliorate ventriculomegaly in a rat model of hydrocephalus. *JCI Insight*. 2020;5(18): e137646.
68. Quintela T, Marcelino H, Deery MJ, Feret R, Howard J, Lilley KS, et al. Sex-related differences in rat choroid plexus and cerebrospinal fluid: a cDNA microarray and proteomic analysis. *J Neuroendocrinol*. 2016. <https://doi.org/10.1111/jne.12340>.
69. Bennett KM, Liu J, Hoelting C, Stoll J. Expression and analysis of two novel rat organic cation transporter homologs, SLC22A17 and SLC22A23. *Mol Cell Biochem*. 2011;352(1–2):143–54.
70. Lang M, Salinin S, Ridder D, Kleesiek J, Hroudova J, Berger S, et al. A transgenic approach to identify thyroxine transporter-expressing structures in brain development. *J Neuroendocrinol*. 2011;23(12):1194–203.
71. Mouse Brain Atlas. <http://mousebrain.org/genesearch.html>. Accessed 15 Dec 2021.
72. Matsumoto N, Kitayama H, Kitada M, Kimura K, Noda M, Ide C. Isolation of a set of genes expressed in the choroid plexus of the mouse using suppression subtractive hybridization. *Neuroscience*. 2003;117(2):405–15.
73. Bernal J, Guadaño-Ferraz A, Morte B. Thyroid hormone transporters—functions and clinical implications. *Nat Rev Endocrinol*. 2015;11(7):406–17.
74. Dolgodilina E, Camargo SM, Roth E, Herzog B, Nunes V, Palacín M, et al. Choroid plexus LAT2 and SNAT3 as partners in CSF amino acid homeostasis maintenance. *Fluids Barriers CNS*. 2020;17(1):17.
75. Nilsson LM, Castresana-Aguirre M, Scott L, Brismar H. RNA-seq reveals altered gene expression levels in proximal tubular cell cultures compared to renal cortex but not during early glucotoxicity. *Sci Rep*. 2020;10(1):10390.
76. Lee JW, Chou CL, Knepper MA. Deep sequencing in microdissected renal tubules identifies nephron segment-specific transcriptomes. *J Am Soc Nephrol*. 2015;26(11):2669–77.
77. Oshio K, Watanabe H, Song Y, Verkman AS, Manley GT. Reduced cerebrospinal fluid production and intracranial pressure in mice lacking choroid plexus water channel Aquaporin-1. *FASEB J*. 2005;19(1):76–8.
78. Pollay M, Hisey B, Reynolds E, Tompkins P, Stevens FA, Smith R. Choroid plexus Na⁺/K⁺-activated adenosine triphosphatase and cerebrospinal fluid formation. *Neurosurgery*. 1985;17(5):768–72.
79. Fahlke C, Fischer M. Physiology and pathophysiology of Cl⁻/K⁺ channels. *Front Physiol*. 2010;1:155.
80. Numata T, Sato-Numata K, Hermosura MC, Mori Y, Okada Y. TRPM7 is an essential regulator for volume-sensitive outwardly rectifying anion channel. *Commun Biol*. 2021;4(1):599.
81. Vrhovac I, Balen Eror D, Klessen D, Burger C, Breljak D, Kraus O, et al. Localizations of Na⁽⁺⁾-D-glucose cotransporters SGLT1 and SGLT2 in human kidney and of SGLT1 in human small intestine, liver, lung, and heart. *Pflugers Arch*. 2015;467(9):1881–98.
82. Chiba Y, Sugiyama Y, Nishi N, Nonaka W, Murakami R, Ueno M. Sodium/glucose cotransporter 2 is expressed in choroid plexus epithelial cells and ependymal cells in human and mouse brains. *Neuropathology*. 2020;40(5):482–91.
83. Chiba Y, Murakami R, Matsumoto K, Wakamatsu K, Nonaka W, Uemura N, et al. Glucose, fructose, and urate transporters in the choroid plexus epithelium. *Int J Mol Sci*. 2020;21(19):7230.
84. Wright EM, Sala-Rabanal M, Ghezzi C & Loo DDF 2018, Sugar Absorption. *Physiology of the Gastrointestinal Tract: Sixth Edition*. Vol. 2–2, Elsevier Inc., pp. 1051–1062.
85. Saisho Y. SGLT2 inhibitors: the star in the treatment of type 2 diabetes? *Diseases*. 2020;8(2):14.
86. Wright EM, Ghezzi C, Loo DDF. Novel and unexpected functions of SGLTs. *Physiology*. 2017;32(6):435–43.
87. Saunders NR, Dziegielewska KM, Møllgård K, Habgood MD, Wakefield MJ, Lindsay H, et al. Influx mechanisms in the embryonic and adult rat choroid plexus: a transcriptome study. *Front Neurosci*. 2015;9:123.
88. Ho HT, Dahlin A, Wang J. Expression profiling of solute carrier gene families at the blood-CSF barrier. *Front Pharmacol*. 2012;3:154.
89. Rouault TA, Zhang DL, Jeong SY. Brain iron homeostasis, the choroid plexus, and localization of iron transport proteins. *Metab Brain Dis*. 2009;24(4):673–84.
90. Marger L, Schubert CR, Bertrand D. Zinc: an underappreciated modulatory factor of brain function. *Biochem Pharmacol*. 2014;91(4):426–35.
91. Herrick-Davis K, Grinde E, Lindsley T, Teitler M, Mancia F, Cowan A, et al. Native serotonin 5-HT_{2C} receptors are expressed as homodimers on the apical surface of choroid plexus epithelial cells. *Mol Pharmacol*. 2015;87(4):660–73.
92. Shipley F, Dani N, Xu H, Deister C, Cui J, Head J, et al. Tracking calcium dynamics and immune surveillance at the choroid plexus blood-cerebrospinal fluid interface. *Neuron*. 2020;108(4):623–639.e10.
93. Mazucanti C, Liu Q, Lang D, Huang N, O'Connell J, Camandola S, et al. Release of insulin produced by the choroid plexis is regulated by serotonergic signaling. *JCI Insight*. 2019;4(23): e131682.
94. Speake T, Kibble JD, Brown PD. Kv1.1 and Kv1.3 channels contribute to the delayed-rectifying K⁺ conductance in rat choroid plexus epithelial cells. *Am J Physiol Cell Physiol*. 2004;286(3):C611–20.
95. Lindvall-Axelsson M, Mathew C, Nilsson C, Owman C. Effect of 5-hydroxytryptamine on the rate of cerebrospinal fluid production in rabbit. *Exp Neurol*. 1988;99(2):362–8.
96. Fisone G, Snyder GL, Fryckstedt J, Caplan MJ, Aperia A, Greengard P. Na⁺, K⁽⁺⁾-ATPase in the choroid plexus. Regulation by serotonin/protein kinase C pathway. *J Biol Chem*. 1995;270(6):2427–30.
97. Angelova K, Puett D, Narayan P. Identification of endothelin receptor subtypes in sheep choroid plexus. *Endocrine*. 1997;7(3):287–93.
98. Schalk KA, Faraci FM, Heistad DD. Effect of endothelin on production of cerebrospinal fluid in rabbits. *Stroke*. 1992;23(4):560–3.
99. Kadel KA, Heistad DD, Faraci FM. Effects of endothelin on blood vessels of the brain and choroid plexus. *Brain Res*. 1990;518(1–2):78–82.
100. Szymdynger-Chodobska J, Chun ZG, Johanson CE, Chodobska A. Distribution of fibroblast growth factor receptors and their co-localization with vasopressin in the choroid plexus epithelium. *NeuroReport*. 2002;13(2):257–9.
101. Panet R, Atlan H. Stimulation of bumetanide-sensitive Na⁺/K⁺/Cl⁻ cotransport by different mitogens in synchronized human skin fibroblasts is essential for cell proliferation. *J Cell Biol*. 1991;114(2):337–42.

102. Johanson CE, Szmydynger-Chodobska J, Chodobski A, Baird A, McMillan P, Stopa EG. Altered formation and bulk absorption of cerebrospinal fluid in FGF-2-induced hydrocephalus. *Am J Physiol.* 1999;277(1):R263–71.
103. Coll G, Arnaud E, Collet C, Brunelle F, Sainte-Rose C, Di Rocco F. Skull base morphology in fibroblast growth factor receptor type 2-related faciocraniosynostosis: a descriptive analysis. *Neurosurgery.* 2015;76(5):571–83.
104. Johanson CE, Donahue JE, Spangenberg A, Stopa EG, Duncan JA, Sharma HS. Atrial natriuretic peptide: its putative role in modulating the choroid plexus-CSF system for intracranial pressure regulation. *Acta Neurochir Suppl.* 2006;96:451–6.
105. Chodobski A, Szmydynger-Chodobska J, Cooper E, McKinley MJ. Atrial natriuretic peptide does not alter cerebrospinal fluid formation in sheep. *Am J Physiol.* 1992;262(5 Pt 2):R860–4.
106. Mori K, Tsutsumi K, Kurihara M, Kawaguchi T, Niwa M. Alteration of atrial natriuretic peptide receptors in the choroid plexus of rats with induced or congenital hydrocephalus. *Childs Nerv Syst.* 1990;6(4):190–3.
107. Speake T, Brown PD. Ion channels in epithelial cells of the choroid plexus isolated from the lateral ventricle of rat brain. *Brain Res.* 2004;1005(1–2):60–6.
108. Uchida Y, Zhang Z, Tachikawa M, Terasaki T. Quantitative targeted absolute proteomics of rat blood-cerebrospinal fluid barrier transporters: comparison with a human specimen. *J Neurochem.* 2015;134(6):1104–15.

Publisher's Note

Springer Nature remains neutral with regard to jurisdictional claims in published maps and institutional affiliations.

Ready to submit your research? Choose BMC and benefit from:

- fast, convenient online submission
- thorough peer review by experienced researchers in your field
- rapid publication on acceptance
- support for research data, including large and complex data types
- gold Open Access which fosters wider collaboration and increased citations
- maximum visibility for your research: over 100M website views per year

At BMC, research is always in progress.

Learn more biomedcentral.com/submissions

